Self-assembly of new porous materials

by

Tia Jacobs

Submitted in partial fulfilment of the requirements for the degree

Doctor of Philosophy

at

Stellenbosch University

Department of Chemistry and Polymer Science

Faculty of Science

Supervisor: Prof. L. J. Barbour

Co-Supervisor: Dr. M. W. Bredenkamp

Date: March 2009

experience significant thermal motion such that only diffuse electron density is observed within the cavity. This is most likely due to weak H:G interactions coupled with the availability of sufficient space to allow such motion. It is interesting to note that even with major deformation (which constitutes an energetic penalty) in the host lattice as it is absorbing acetylene (Figure 4.20), the gas uptake reaction is still energetically favoured. This is in contrast to the CO_2 sorption behaviour, where no noteworthy deformation appears to be necessary (Figure 4.23) and thus no structural energetic penalty is incurred for gas uptake, although a lower occupancy relative to that observed for C_2H_2 is still observed at similar overpressures. This difference in sorption behaviour can most likely be ascribed to differences in the H:G stabilisation energies of the two different gases and, in the case of C_2H_2, the stabilisation energy probably compensates for the deformation energy. Note that the "gates" between successive voids dilate slightly with increasing CO_2 gas pressure, which is opposite to what is observed for C_2H_2.

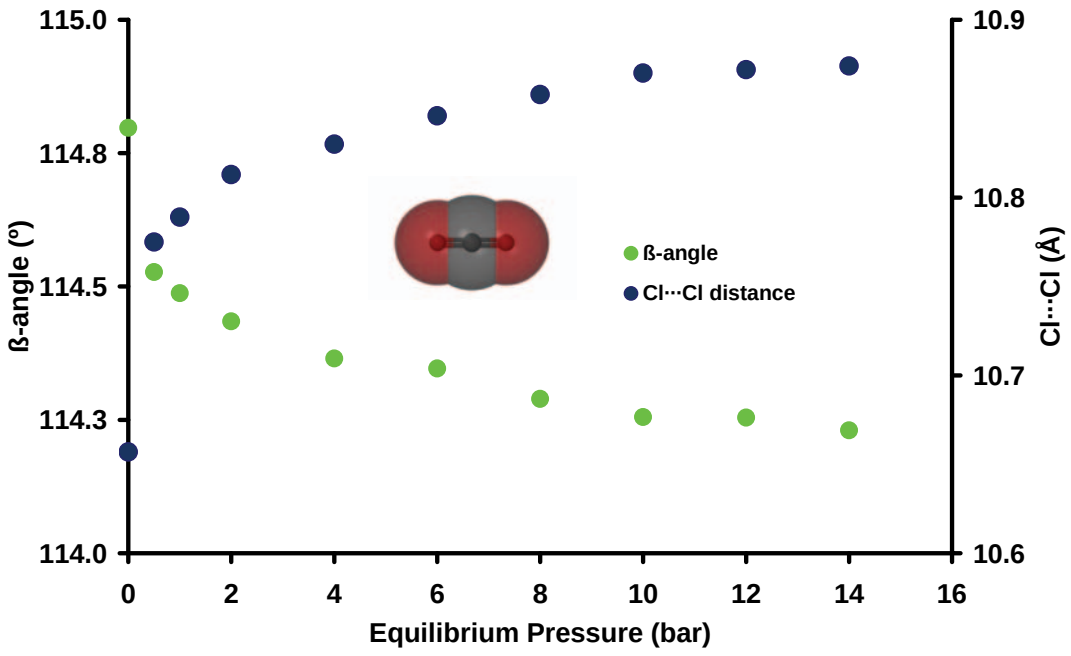

Figure 4.23 β-angle and Cl···Cl distance in CO_2 structures of **15** determined at different equilibrium pressures. The distortion in the host framework is not as substantial as that observed during the sorption of C_2H_2 by **15**.

When comparing the gas uptake data of CO_2 determined using the two independent methods (*i.e.* gravimetric sorption analysis and electron counting), the occupancy values agree at pressures up to about 8 bar (Figure 4.24). However, at higher pressures the electron count values are slightly lower, most likely as a result of equilibrium not being reached before measurement of the X-ray data.

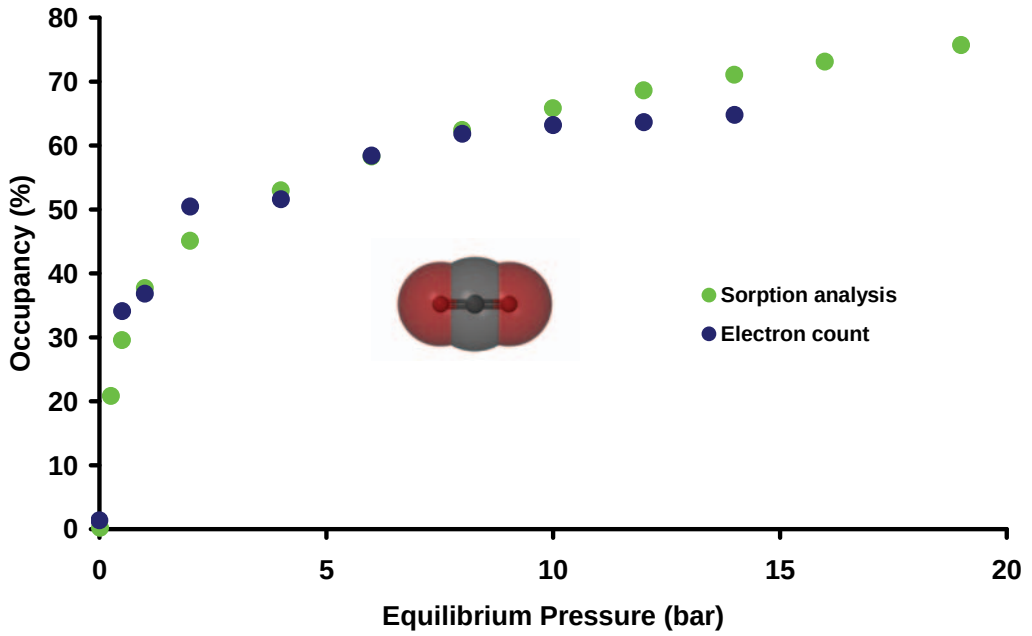

Figure 4.24 Gas occupancy as a function of pressure for the sorption of carbon dioxide by **15**, determined at 22 ºC from gravimetric sorption analysis and electron density counts from single-crystal X-ray diffraction.

In order to compare structural changes and host:guest interactions of metallocycle **15** with those of metallocycle **16**, analogous X-ray and gas sorption experiments were conducted using **16** and carbon dioxide. Single-crystal diffraction data were collected at 22 °C under vacuum and CO_2 pressures of 1, 2, 4, 8 12, 16 and 19 bar. From the gravimetric gas sorption experiment it is evident that **15** has the greater affinity for CO_2. Indeed, **15** reaches 50% occupancy at an equilibrium pressure of 4 bar, whereas **16** only reaches a similar occupancy at *ca* 16 bar. After structure elucidation of the series under increasing equilibrium pressures of CO_2, the changes in certain lattice parameters of **16** were investigated as a function of pressure (Figure 4.25). From this study it is evident that the guest interacts very weakly with the host as there is relatively little change in the $I^-\cdots I^-$ distance (10.354(2) to 10.489(3) Å) as the pressure is increased. The β-angle is also poorly correlated to the equilibrium pressure. As

with the $\mathbf{15_{CO2}}$ room temperature structures, CO_2 atomic coordinates could not be modelled in all but one of the iodide analogues. In an attempt to obtain CO_2 coordinates, intensity data were collected under similar conditions as for the full-occupancy structure of $\mathbf{15_{CO2}}$ (*i.e.* 233 K, 10 bar). At this temperature and pressure, only diffuse electron density was observed for **16** and 25.9 electrons per cavity were counted using SQUEEZE – which corresponds to an occupancy of 59%. However, it was possible to model the guest molecule in $\mathbf{16_{16,CO2}}$ sensibly (16 bar, 22 ºC). In this structure, an electron count of 22.3 was obtained, corresponding to *ca* one CO_2 molecule per cavity. The guest was located in the centre of the cavity with the C atom situated on the 2/*m* site. There is apparently no van der Waals interaction between guest and host (this statement considers the van der Waals radius of iodine and iodide, Figure 4.26). This is reflected in the insignificant change in lattice parameters (as discussed for Figure 4.25) and a volume that only increases by *ca* 2 $Å^3$ from $\mathbf{16_{vac}}$ to $\mathbf{16_{16,CO2}}$. The CO_2 molecule is almost parallel to the $I^-\cdots I^-$ vector across the length of the cavity, with $\angle$C-O$\cdots I^-$ = 174.1º.

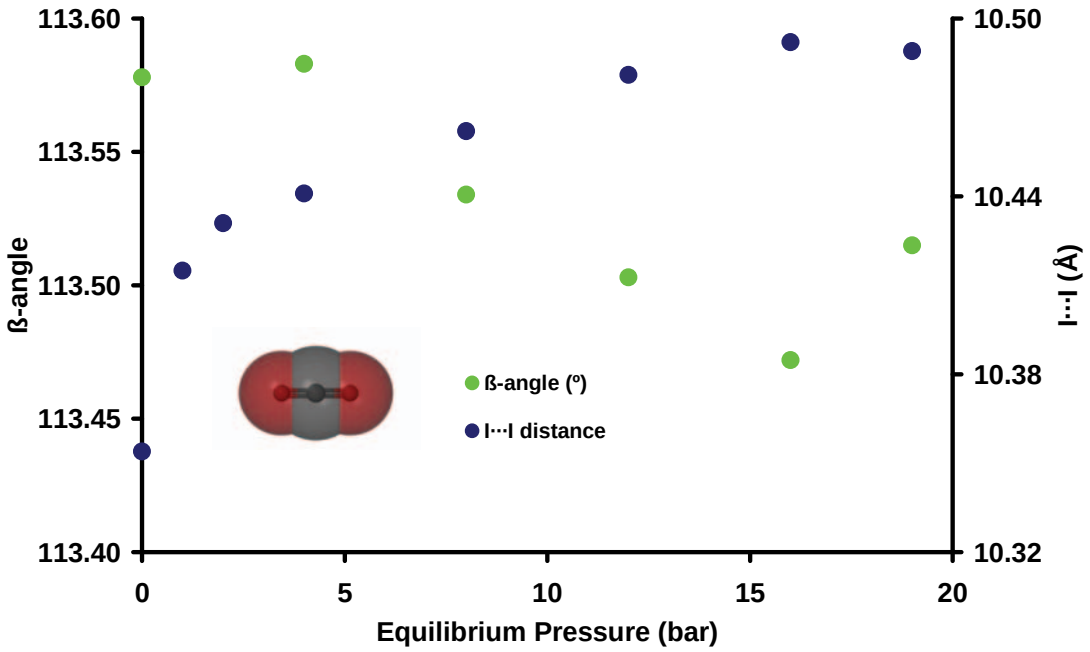

Figure 4.25 β-angle and I···I distance in CO_2-loaded structures of **16.**

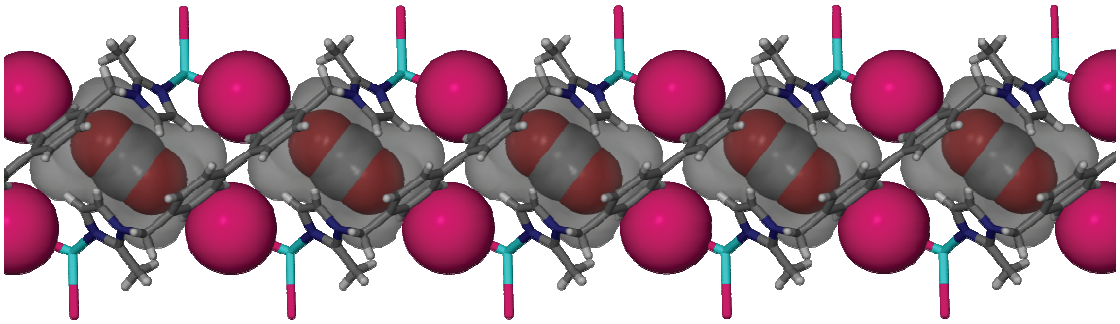

Figure 4.26 Structure of $\mathbf{16}_{\mathbf{16,CO2}}$ determined at 16 bar and 22 ºC. The guest-accessible cavities are shown as semi-transparent grey surfaces with the host metallocycles and neighbouring carbon dioxide molecules shown in capped-stick representation. The iodide anions forming the floor and roof of the mapped cavity are shown in space-filling representation along with the CO_2 molecules. The CO_2 molecules are positioned parallel to the I···I vector across the cavity and the volume of each guest-accessible void is approximately 126 $Å^3$.

An overlay of the two occupancy curves shows that occupancies determined from the electron count in the single-crystal structures are only slightly higher than those determined by gravimetric sorption analysis. This may be due to phase purity problems with the sample used for gravimetric sorption analysis.

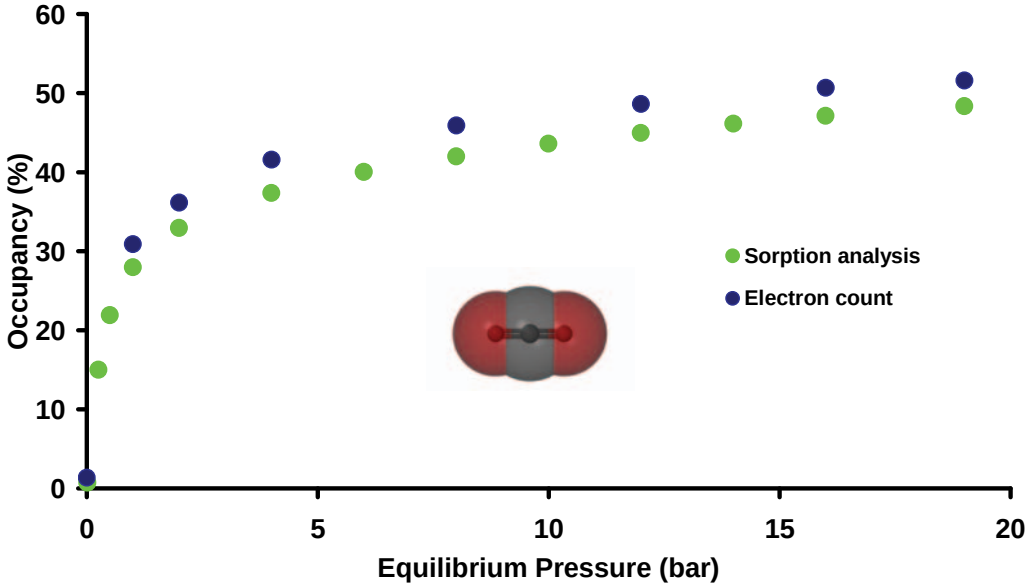

Figure 4.27 Gas occupancy as a function of pressure for the sorption of carbon dioxide by **16**, determined at 22 ºC from gravimetric sorption analysis (•) and electron counting (•) from single-crystal X-ray diffraction.

In summary, the processes of C_2H_2 and CO_2 sorption by **15** and CO_2 sorption by **16** was followed closely using single-crystal X-ray diffraction. Valuable information

was gained about the specific host:guest and guest:guest interactions. These structural parameters could be used to calculate intermolecular energies for interactions such as $Cl^{-}\cdots H–C\equiv C–H$ (in $\mathbf{15_{C2H2}}$), making it possible to rationalise the deformation due to guest uptake. This information can also explain the difference in CO_2 sorption behaviour between **15** and **16**, where a $Cl^{-}\cdots C(\delta^{+})$ interaction is apparent in **15**, but no discernible $I^{-}\cdots C(\delta^{+})$ interaction occurs in **16**. The above serves to illustrate that important information can be gleaned from the abundance of evidence obtainable from such complementary studies.

Pertinent data obtained from the structure determinations of **15** and **16** under controlled pressures of different gases is summarised in Tables 4.1 to 4.4. These data emphasise the amount of structural information obtainable from such a series of systematic measurements. Atomic numbering used in Tables 4.1 to 4.4 (and later in table 4.5) is given in Figure 4.28.

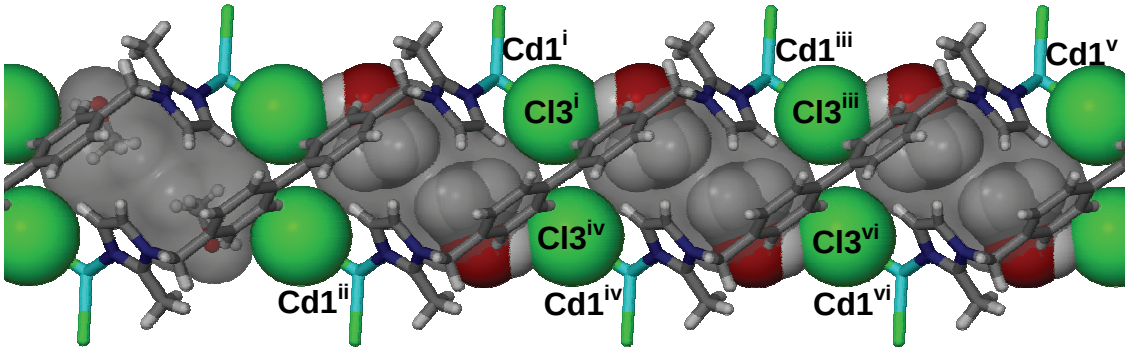

Figure 4.28 Atomic numbering of relevant atoms of **15** in Tables 4.1 to 4.4 showing changes in size and shape of the void bounded by $Cl3^{i}$ and $Cl3^{vi}$ and $Cd1^{iii}$ and $Cd1^{iv}$. For structures of **16**, the labels remain identical and $Cl3^{superscript}$ can be substituted by $I3^{superscript}$.